

Neurofascins Are Required to Establish Axonal Domains for Saltatory Conduction Report

Diane L. Sherman,¹ Steven Tait,¹ Shona Melrose,¹ Richard Johnson,¹ Barbara Zonta,¹ Felipe A. Court,¹ Wendy B. Macklin,² Stephen Meek,³ Andrew J.H. Smith,³ David F. Cottrell,¹ and Peter J. Brophy^{1,*}

¹Centre for Neuroscience Research
University of Edinburgh
Edinburgh EH9 1QH
United Kingdom

²Department of Neurosciences
The Lerner Research Institute, NC30
The Cleveland Clinic Foundation
Cleveland, Ohio 44195

³Gene Targeting Laboratory
Institute for Stem Cell Research
University of Edinburgh
The King's Buildings
Edinburgh EH9 3JQ
United Kingdom

Summary

Voltage-gated sodium channels are concentrated in myelinated nerves at the nodes of Ranvier flanked by paranodal axoglial junctions. Establishment of these essential nodal and paranodal domains is determined by myelin-forming glia, but the mechanisms are not clear. Here, we show that two isoforms of Neurofascin, Nfasc155 in glia and Nfasc186 in neurons, are required for the assembly of these specialized domains. In Neurofascin-null mice, neither paranodal adhesion junctions nor nodal complexes are formed. Transgenic expression of Nfasc155 in the myelinating glia of *Nfasc*^{-/-} nerves rescues the axoglial adhesion complex by recruiting the axonal proteins Caspr and Contactin to the paranodes. However, in the absence of Nfasc186, sodium channels remain diffusely distributed along the axon. Our study shows that the two major Neurofascins play essential roles in assembling the nodal and paranodal domains of myelinated axons; therefore, they are essential for the transition to saltatory conduction in developing vertebrate nerves.

Introduction

A distinguishing feature of complex nervous systems is their ability to transmit nerve impulses rapidly by saltatory conduction. Transition to this mode of conduction during vertebrate development requires the establishment of distinct axonal domains under the influence of myelin-forming glia (Poliak and Peles, 2003; Ranvier, 1875; Salzer, 2003; Sherman and Brophy, 2005). Voltage-gated sodium channels cluster at high density at nodes of Ranvier between the ensheathing glia, thus causing the depolarizing action potential to be propagated discontinuously and rapidly. Flanking the nodes are the

paranodal junctions between axon and glia. Both paranodal junctions and nodes must be intact to support saltatory conduction (Poliak and Peles, 2003; Salzer, 2003). However, in spite of considerable progress in determining the molecular constitution of the nodes and paranodes, it is by no means clear how oligodendrocytes and Schwann cells in the central and peripheral nervous systems (CNS and PNS) initiate their assembly. In this study, we have investigated the role of two alternatively spliced products of the *Neurofascin* (*Nfasc*) gene, Nfasc186 and Nfasc155, in establishing these domains.

In addition to voltage-gated channel proteins, the nodal complex also contains the transmembrane proteins NrCAM and Nfasc186 (Davis et al., 1996; Tait et al., 2000) together with proteins that are presumed to link them to the actin cytoskeleton, namely β IV-spectrin and ankyrinG (Jenkins and Bennett, 2002; Komada and Soriano, 2002; Lacas-Gervais et al., 2004). Although there is indirect evidence that neuronal Nfasc186 has a role in the assembly of the nodal complex, NrCAM does not appear to be essential (Custer et al., 2003; Lambert et al., 1997; Lustig et al., 2001). Analysis of the sequence of events at the nodal complex has suggested that Neurofascin and NrCAM are first detectable at sites presumed to be nascent nodes of Ranvier and that ankyrinG and voltage-gated sodium channels subsequently cluster with these cell adhesion molecules (Lambert et al., 1997).

Flanking the nodes are the septate-like junctions between the ensheathing glial cell and the axon composed of the axonal adhesion proteins Caspr (also known as Paranodin) and Contactin in a *cis* complex (Bhat et al., 2001; Boyle et al., 2001; Einheber et al., 1997; Gollan et al., 2003; Menegoz et al., 1997). The glial isoform of Neurofascin, Nfasc155, resides on the glial side of the junction and has been shown to bind to the Caspr-Contactin complex *in vitro* (Charles et al., 2002; Tait et al., 2000). Hence, Nfasc155 seems to be an excellent candidate as a glial component of the paranodal adhesion complex. The specific axonal protein with which Nfasc155 interacts is likely to be Contactin (Gollan et al., 2003); nevertheless, axoglial junctions are disrupted in the absence of either Caspr or Contactin because the complementary *cis*-interacting axonal protein is also lost from the paranode (Bhat et al., 2001; Boyle et al., 2001). The loss of Contactin at the paranode when Caspr expression is ablated may be explained by the former's dependence on Caspr for delivery to the plasma membrane (Favre-Sarrailh et al., 2000; Gollan et al., 2003). In contrast to the mutual dependence of Caspr and Contactin for each other's delivery to the paranodal axoglial junction, Nfasc155 is still detectable at the paranodes in the absence of the Caspr-Contactin complex (Bhat et al., 2001; Boyle et al., 2001). Hence, it is still not certain that Nfasc155 is a bona fide component of the axoglial junctional complex.

Here, we show how Nfasc155 and Nfasc186 play distinct and essential roles in the formation of functional nodes of Ranvier. Glial Nfasc155 is essential for the assembly of the paranodal axoglial junction. However,

*Correspondence: peter.brophy@ed.ac.uk

stable concentration of sodium channels at the nascent node requires the neuronal isoform of Neurofascin, Nfasc186. We propose that differential expression of *Nfasc* in glia and neurons plays a fundamental role in the switch to saltatory conduction, thus ensuring rapid conduction in the mature vertebrate nervous system.

Results and Discussion

Phenotype of *Nfasc*^{-/-} Mice

To test the role of the Neurofascins Nfasc186 and Nfasc155 in domain segregation at the node and paranode, we inactivated the *Nfasc* gene by homologous recombination in ES cells (Figures 1A and 1B). Homozygous Nfasc-null animals were born at expected Mendelian ratios with a normal appearance, but they died suddenly at 6–7 days after birth when the postnatal transition to saltatory conduction is occurring in the CNS and PNS. Henceforth, we were careful to take animals before they demonstrated any obvious clinical phenotype, and we subsequently identified Nfasc-null animals by genotyping. Western blotting confirmed the complete ablation of Nfasc186 and Nfasc155 expression (Figure 1C). Interestingly, the total amounts of Caspr, Contactin (both paranodal proteins), voltage-gated sodium channels, or NrCAM (both nodal proteins) were not reduced in the absence of the Neurofascins in PNS axons (Figure 1D). Further, the amount of peripheral myelin appeared to be unaffected as judged by Western blotting for the major myelin protein P0 (Figure 1D).

Light microscopy of transverse sections of sciatic nerves confirmed that the myelin sheath in Neurofascin-null animals was grossly normal (Figure 2A). Nevertheless, the conduction velocities of mutant peripheral sciatic nerves were drastically reduced from 3.7 ± 0.5 m/s (wild-type) to 0.7 ± 0.2 m/s (*Nfasc*^{-/-}) (means \pm SEM; $n = 3$ for each). The rates of nerve conduction in the mutants were reminiscent of those typical for unmyelinated axons, in which sodium channels are diffusely spread along the axon. Hence, we determined the effect of the absence of Neurofascins at the node and paranode on the localization of other components of these two domains. Absence of Nfasc155 from the paranode caused the loss of both Caspr and Contactin from the junction. And without Nfasc186 at the node of Ranvier, other major components of the nodal complex, sodium channels, NrCAM, AnkyrinG, or β IV-spectrin were no longer concentrated at the node (Figure 2B). Because we had shown that the amounts of most of these proteins were unaffected in the *Nfasc*^{-/-} nerve (Figure 1D), this suggested that the primary role played by both Nfasc155 and Nfasc186 was to ensure that their respective paranodal and nodal complexes are appropriately assembled. The disruption of the paranodal and nodal proteins observed in the PNS was equally demonstrable in the CNS (data not shown).

The absence of intact axoglial structures at the paranode was reflected by the loss of septate junctions and a widening of the junctional gap from 16.3 ± 0.1 nm (wild-type) to 26.0 ± 0.5 nm (*Nfasc*^{-/-}) (mean \pm SEM; $n = 3$ each) (Figure 2C). Disruption of the axoglial junction apparently allowed the microvillar processes of Schwann cells to interdigitate in the gap between axon and glial cell (Figure 2C). This type of derangement

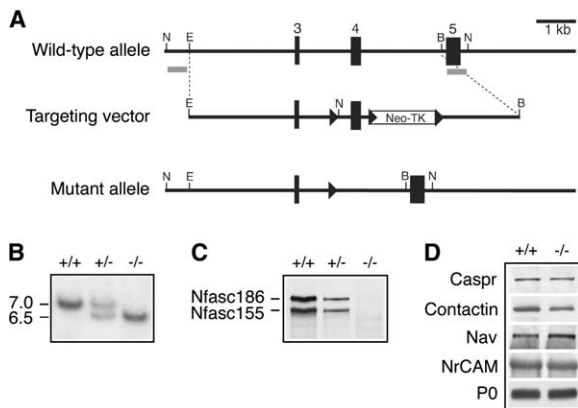


Figure 1. Generation of Neurofascin Mutant Mice

(A) Schematic diagram of the wild-type *Nfasc* gene, targeting vector, and mutant allele after Cre-mediated excision. Deletion of exon 4 in the targeted allele by Cre recombination was predicted to result in a transcript with an exon 3 to 5 splice junction and consequent in-frame stop codon in exon 5. The positions of the 5' and 3' probes external to the targeting vector used for Southern blotting are shown. N, NcoI; E, EhoI; B, BamHI.

(B) Southern blot analysis of tail genomic DNA from intercrossing two heterozygous mutants. DNA was digested with NcoI and analyzed with the 5' probe. The sizes of the wild-type and mutant fragments are 7.0 and 6.5 kb, respectively.

(C) Western blot analysis of sciatic nerve homogenates from wild-type, *Nfasc*^{+/-}, and *Nfasc*^{-/-} mice, respectively, showing the absence of both major Nfasc186 and Nfasc155.

(D) Western blot of components of the paranodal junction (Caspr; Contactin), the nodal complex (voltage-gated sodium channels, Nav; NrCAM), and myelin (P0) showing that the absence of the Neurofascins does not affect the amounts of these major proteins of the paranodal and nodal complexes or myelin in the peripheral nerves of mutant mice.

has also been observed at the disrupted axoglial junctions of peripheral axons in mice lacking a functional *Caspr* gene (Bhat et al., 2001).

Elimination of NrCAM simply delays sodium-channel clustering, and loss of β IV-spectrin does not completely prevent sodium channels concentrating at the nodes of Ranvier (Custer et al., 2003; Komada and Soriano, 2002; Lacas-Gervais et al., 2004). Hence, it appears that the Neurofascins are uniquely important in the mechanisms underlying the assembly of the nodal apparatus. Similarly, although the absence of either Caspr or Contactin prevents the targeting of its *cis* binding partner in the axonal membrane to the paranode, neither is essential for the localization of glial Nfasc155 (Bhat et al., 2001; Boyle et al., 2001). Hence, glial Neurofascin can be targeted to the paranode without the requirement for *trans* interactions with the axonal Caspr-Contactin complex. In contrast, without paranodal Nfasc155, neither Caspr nor Contactin is targeted to the paranode. This points to a possible pioneering role for the Neurofascins in axoglial junction formation as well as in node assembly.

Extracellular Domain of Nfasc155 Rescues the Paranodal Complex

We have previously shown that the extracellular domain of Nfasc155 alone is sufficient for strong interaction with the Caspr-Contactin complex *in vitro* (Charles et al., 2002). Hence, to test if the extracellular domain of

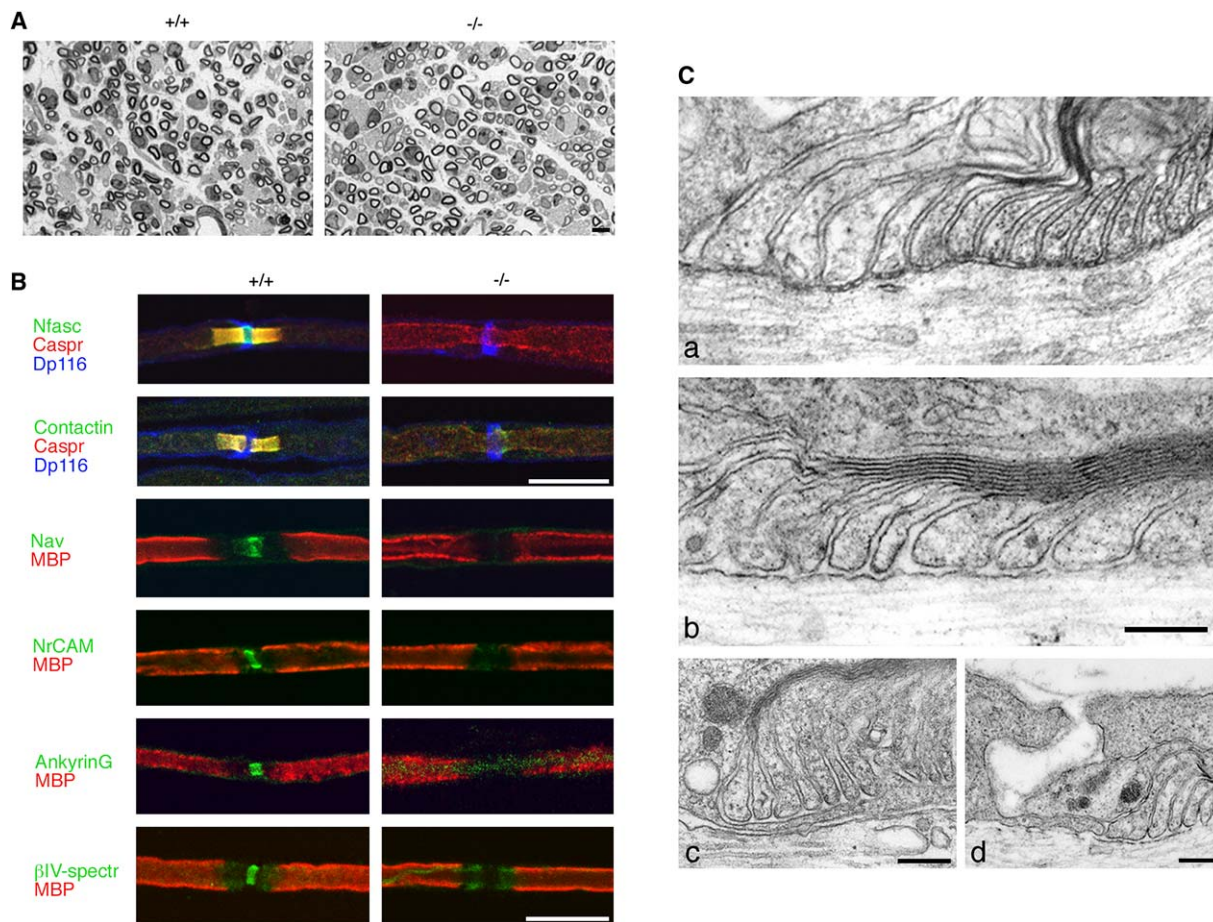


Figure 2. Disruption of the Paranodes and Nodes in Neurofascin Mutant Mice

(A) Resin sections (1 μ m) from the sciatic nerves of 7 day old *Nfasc*^{+/+} and *Nfasc*^{-/-} animals were compared by light microscopy. There were no obvious differences in either the number or thickness of myelin sheaths at this age. Scale bar, 5 μ m.

(B) Immunofluorescence analysis of *Nfasc*^{+/+} and *Nfasc*^{-/-} animals showed that the axoglial junctional components Caspr and Contactin were no longer concentrated at the paranodes. Immunostaining of teased fibers for the major isoform of Dystrophin expressed in Schwann cells (Dp116) was used to localize the node of Ranvier because it is concentrated in the nodal microvilli. Immunostaining for Nfasc with a pan anti-Neurofascin antibody recognized Nfasc186 at the node and Nfasc155 at the paranode in wild-type mice. Both were absent in mutants. The nodal components, voltage-gated sodium channels (Nav) NrCAM, AnkyrinG, and β IV-spectrin (β IV-spectr) were also not clustered at the node in mutant animals. The myelin sheath was visualized by immunostaining for myelin basic protein (MBP). Scale bars, 10 μ m.

(C) Electron microscopy of the paranodes in wild-type and mutant mice. Septate junctions are clearly visible at the axoglial junctions of wild-type animals (a), whereas in mutant paranodes, the septate junctions are no longer present, and there is a larger gap between the base of the paranodal loops and the axolemma (b). Note the normal appearance of the overlying myelin sheath in the mutant (b). Disruption of the axoglial junctions at deranged paranodes resulted in the interdigitation of Schwann cell processes between the same Schwann cell and the underlying axon (c) and between the paranodal loops of adjacent Schwann cells and the axolemma (d). Scale bars, 0.2 μ m.

*Nfasc*155 could rescue the axoglial junction in vivo, we generated transgenic mice expressing *Nfasc* Δ IC comprising the complete extracellular and transmembrane domains of *Nfasc*155, and the first 13 of the 110 amino acid cytoplasmic tail linked to a FLAG tag. This protein therefore lacks most of the C-terminal domain, including the ankyrin binding site (Davis and Bennett, 1993). First, we showed that this protein was delivered to the plasma membrane in transfected HeLa cells (Figure 3A), and transgenic expression of *Nfasc* Δ IC in oligodendrocytes and Schwann cells showed that the protein was targeted to the paranodes in mouse CNS and PNS (Figure 3B). Targeting of the extracellular domain of *Nfasc*155 to the glial paranodal membranes allowed us to test if this could reconstitute the axoglial junctional complex in *Nfasc*^{-/-}/*Nfasc* Δ IC⁺ mice. The presence of the extracel-

lular domain of *Nfasc*155 could indeed recruit Caspr and Contactin to the paranode (Figure 3C). Contactin always accompanied Caspr at the rescued paranodes. This supports the view that *Nfasc*155 has a crucial role in the formation of the axoglial junction.

Intact Paranodal Junctional Complexes Do Not Rescue the Node

The role, if any, of the axoglial junction in the formation of the node is still uncertain (Poliak and Peles, 2003; Salzer, 2003). Hence, it was of considerable interest to determine if rescue of the paranodal complex of Caspr-Contactin with the extracellular domain of *Nfasc*155 influenced the clustering of sodium channels at the node. We measured fluorescence pixel intensities at the nodes of Ranvier in wild-type and *Nfasc*^{-/-} mice after immunostaining for

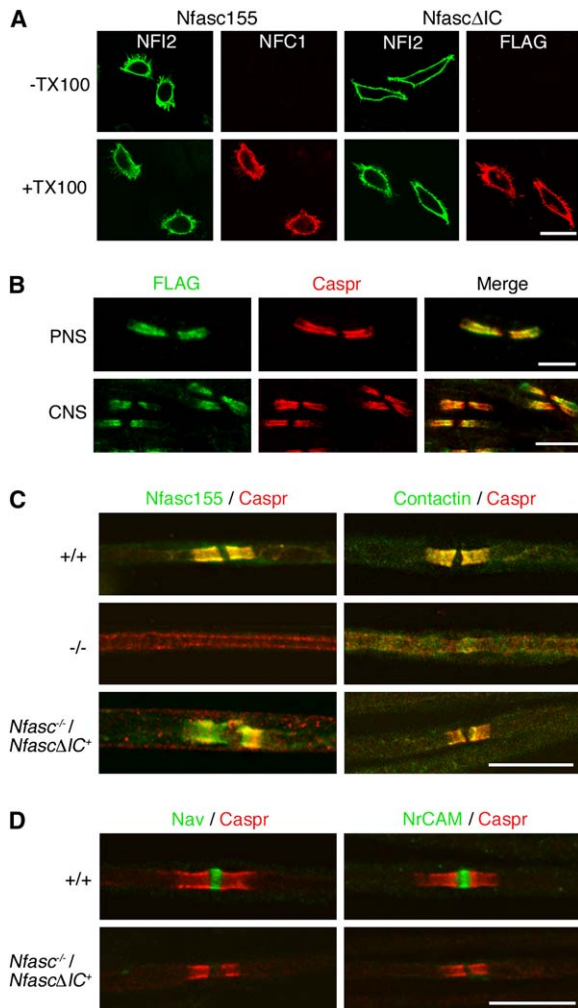


Figure 3. Reformation of the Paranodal Adhesion Complex Does Not Rescue the Node

(A) A truncated form of Nfasc155, Nfasc155ΔIC, in which most of the cytoplasmic tail was replaced with a FLAG tag was expressed in HeLa cells. Cells were immunostained with anti-FLAG or NFI2 antibody that recognizes the extracellular domain without (–) or after (+) permeabilization of the cells with 0.1% (w/v) Triton X-100. Confocal microscopy showed that the mutated protein was delivered to the cell surface. Control cells expressing wild-type protein (Nfasc155) were stained with NFI2 and the NFC1 antibody, which recognizes the extreme C terminus of Nfasc155.

(B) Immunostaining of teased fibers in the PNS and sections of CNS shows that Nfasc155ΔIC is targeted to the paranodes in myelinated axons.

(C) Immunostaining of teased fibers shows that Nfasc155ΔIC expressed on a neurofascin-null background reconstitutes the paranodal adhesion complex with Contactin and Caspr.

(D) Formation of the paranodal adhesion complex does not rescue the nodal components, voltage-gated sodium channels (Nav), or NrCAM in the absence of Nfasc186. All scale bars, 10 μm.

sodium channels and compared them with nodes flanked by paranodes in which the paranodal complex had been reconstituted in *Nfasc*^{–/–}/*Nfasc*ΔIC⁺ mice. The intensity of sodium-channel staining at wild-type nodes (14.93 ± 0.30) was significantly different to that of both the *Nfasc*^{–/–} (4.43 ± 0.69) and *Nfasc*^{–/–}/*Nfasc*ΔIC⁺ (4.28 ± 0.33) mice (means ± SEM, *p* < 0.001; Mann-Whitney test, minimum of 50 nodes and two animals per condition).

However, there was no significant difference between *Nfasc*^{–/–} and *Nfasc*^{–/–}/*Nfasc*ΔIC⁺ mice (Figure 3D). In similar experiments, NrCAM, another nodal component that is also believed to interact with sodium channels, was also not clustered at the node after reconstitution of the paranodal complex (Figure 3D) (McEwen and Isom, 2004). This supports a crucial role for Nfasc186 in assembling the nodal complex.

Implications for the Assembly of Paranodes and Node of Ranvier

Voltage-gated sodium channels remain largely confined to the node of Ranvier even when the axoglial junction is disrupted in mice lacking either Caspr (Bhat et al., 2001) or Contactin (Boyle et al., 2001). This is consistent with the conclusion from the present work that disruption of the nodal complex in *Nfasc*^{–/–} mice is not a result of disordering the paranode but is rather due to the absence of Nfasc186. Indeed, there is already substantial evidence that Nfasc186 has a significant role in the early stages of node assembly (Bennett and Lambert, 1999; Lambert et al., 1997; Lustig et al., 2001). A pioneering role for NrCAM in node formation has also been proposed, although sodium channels can still cluster at PNS nodes in the absence of NrCAM, albeit with a significant delay (Custer et al., 2003; Sakurai et al., 2001).

Transgenic expression of the extracellular domain of Nfasc155 at the paranode showed that reconstitution of the paranodal complex did not significantly promote the assembly of the nodal complex, as judged by the localization of voltage-gated sodium channels or NrCAM. Does this mean that the paranodal axoglial junction has no role in the assembly or stabilization of the node of Ranvier? Elimination of Caspr results in a more diffuse distribution of sodium channels at the node, which is consistent with the view that the axoglial junction has a sieve or barrier-like function with respect to the mobility of nodal constituents (Bhat et al., 2001; Pedraza et al., 2001). However, peripheral nerves lacking Contactin have normal sodium-channel distributions at the node (Boyle et al., 2001). Nevertheless, it does seem likely that axoglial-junction integrity influences aspects of nodal function, particularly with respect to the developmentally regulated switch in sodium-channel type expressed at the node (Boiko et al., 2001; Pedraza et al., 2001).

A provocative model that incorporates a key role for the *Nfasc* gene in establishing essential axonal domains in response to axon-glia interaction during myelination proposes that Nfasc155 directs the formation of the paranodal junction, whereas an Nfasc186-NrCAM complex pioneers the assembly of the nodal complex, as first proposed by Salzer and colleagues (Lustig et al., 2001) (Figure 4). Recent evidence suggests that as well as interacting with AnkyrinG, Nfasc186 can also interact directly with sodium-channel subunits (McEwen and Isom, 2004). Furthermore, Nfasc186 can interact in trans with gliomedin, a recently described component of the Schwann cell microvilli that overlies the node of Ranvier (Eshed et al., 2005). Gliomedin may first anchor Nfasc186 at the nascent node, after which Nfasc186 has all the attributes to serve as both a pioneer and a stabilizer of the nodal complex, which is in keeping with its essential role found in this work.

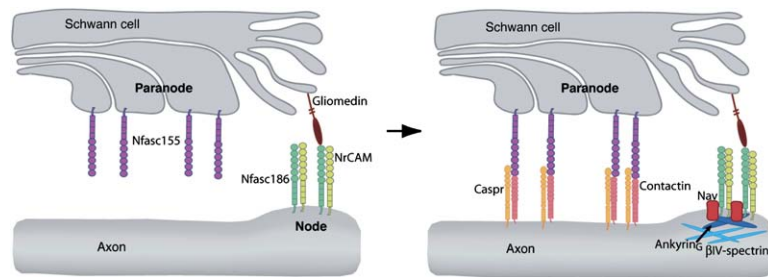


Figure 4. Model Depicting the Potential Role of the Neurofascins in Establishing the Nodal and Paranodal Domains in the PNS

Nfasc155 is delivered to the paranodal regions independently of Caspr and Contactin, whereas the delivery of Nfasc186, together with NrCAM, may be accompanied by or dependent on gliomedin expressed in the microvilli. Once located at the paranodes and nodes, respectively, Nfasc155 and the Nfasc186/NrCAM complex recruit their binding partners to form the paranodal and nodal complexes.

Experimental Procedures

Generation of *Nfasc* Mutant Mice

Nfasc^{-/-} mice were generated by homologous recombination in E14-TG2a.IV (129/Ola strain) ES cells by methods described previously (Gillespie et al., 2000). The replacement targeting vector contained three *loxP* sequences in the same orientation. The first *loxP* sequence was inserted at an *Apal* site in intron 3, 262 bp upstream of exon 4, and the two other *loxP* sequences, which flanked a PGKneo-HSVtk positive-negative selection cassette, were introduced at a *Scal* site in intron 4 located 130 bp downstream of the end of exon 4. For the initial targeting, ES cells were selected in G418 only, and resistant clones screened by Southern blot analysis of *NcoI* digested genomic DNA by hybridization probes external to and flanking the 5' and 3' vector homology arms. The 5' probe (450 bp *NcoI*-*EheI* fragment) and the 3' probe (*Bam*HI-*NcoI* fragment) both detected a 7.0 kb fragment corresponding to the wild-type allele and 4.2 kb and 3.0 kb fragments, respectively, corresponding to the targeted allele. A targeted clone was expanded in nonselective medium and transfected with the supercoiled Cre recombinase-expression plasmid pCAGGS-Cre-IRES^{puro} to generate cells with a deletion of both exon 4 and the selection cassette. Transfected cells were passaged in nonselective medium for 7 days and then plated at a density of 10⁴ cells per 10 cm plate in medium containing 2.5 μM ganciclovir. After selection for 5 days, ganciclovir-resistant clones were recovered and then screened by Southern blot analysis of their genomic DNA with the same combination of restriction digestion and hybridization probes as above. Two clones were identified with the correct excision of exon 4 and the PGKneo-HSVtk cassette as evidenced by the presence of a new 6.5 kb fragment detected with both 5' and 3' probes and loss of the 4.2 kb and 3.0 kb fragments. Both clones gave good germline-transmitting chimeras in test crosses with the C57BL/6 strain, and offspring heterozygous for the targeted exon deletion were subsequently identified by tail biopsy and Southern blot analysis as above. Heterozygotes were backcrossed onto the C57BL/6 background for at least six generations prior to experimental analysis.

Transgenic mice expressing a truncated form of Nfasc155 were generated by pronuclear injection by methods previously described (Sherman and Brophy, 2000). A cDNA encoding amino acids 1 to 1073 of the Nfasc155 sequence that included all the extracellular domain, the transmembrane segment and 13 amino acids of the cytoplasmic tail was fused at its 3' end to the FLAG tag sequence (*Nfasc*ΔIC) and inserted in the pPLP-SV40/bluescript vector carrying the proteolipid protein promoter known to drive expression of downstream sequences in both oligodendrocytes and Schwann cells (Wight et al., 1993). A line was selected that displayed robust expression of NfascΔIC in both oligodendrocytes and myelinating Schwann cells. After backcrossing to a C57BL/6 background for at least six generations, this was interbred with *Nfasc*^{+/-} mice to generate *Nfasc*^{-/-}/*Nfasc*ΔIC⁺ mice.

Antibodies, Microscopy, and Western Blots

Unless indicated otherwise, all microscopy images were from nerves of 7 day old animals. For teased fiber preparation, quadriceps nerves were removed and fixed for 30 min in 4% paraformaldehyde, 0.1 M sodium phosphate buffer (pH 7.4), washed in several changes of phosphate buffer, and teased on 3-aminopropyltriethox-

ysilane (TESPA)-coated slides. Primary antibodies were used at the following dilutions: rabbit NFC1 (pan anti-Neurofascin C terminus, 1:2000) (Tait et al., 2000); rabbit NFF3 (anti-third fibronectin type III domain of Nfasc155, 1:2000) (Tait et al., 2000); rabbit NFI2 (anti-extracellular domain of Nfasc155-aa NNPYDSSLRNHPDIYSAR in exon 3, 1:100); rabbit anti-FLAG (1:400); mouse anti-FLAG (1:300) (Sigma); guinea pig anti-Caspr (1:200), (Tait et al., 2000) (Dr. D.R. Colman); rabbit anti-MBP (1:1000), (Vouyiouklis and Brophy, 1993); rabbit anti-NrCAM (anti-intracellular domain-aa DAHADPEIQPMK, 1:200); rabbit anti-Contactin (1:500), chicken anti βIV-spectrin (1:200) (Komada and Soriano, 2002); mouse anti AnkyrinG (Oncogene, 1:50); mouse pan anti-sodium channel (IgG1, 1:300) (Dr. M. Rasband); mouse anti-dystrophin (1:100), (MANDRAI, Sigma). The secondary antibodies were goat FITC-conjugated anti-rabbit IgG (1:200), (Cappel); donkey FITC-conjugated anti-chicken IgY (1:200); donkey TRITC-conjugated anti-guinea pig IgG (1:200) (all Jackson Immunoresearch); goat TRITC-conjugated anti-mouse IgG1 (1:200) (Southern Biotech); and goat AlexaFluor 647-conjugated anti-mouse IgG1 (1:200) (Molecular Probes). Nerves were prepared for electron microscopy as described previously (Gillespie et al., 2000). Quantitation of pixel density of confocal images immunostained for sodium channels was performed with a Leica TCL-SL confocal microscope and Leica proprietary software. The nodal region of interest (ROI) for each node was defined as the space between the limits of the myelin sheath as determined by costaining for MBP. Background pixel intensity measured in the same size ROI at the center of the same internodal axon was subtracted. Western blotting was performed as described with between 5- to 10-fold-higher dilutions of antibodies than were used for immunostaining (Gillespie et al., 1994). Rabbit anti-P0 (1:5000) (Dr. D.R. Colman) was used exclusively for Western blotting.

Electrophysiology

Acutely prepared sciatic nerves, taken from 7 day old wild-type and mutant mice were placed in oxygenated Krebs's solution, and conduction velocities were measured as described (Court et al., 2004).

Transfections

The Nfasc155ΔIC fusion protein and the wild-type protein Nfasc155 were expressed by transfection in HeLa cells with the pCDNA3 expression vector. Transfection and culture conditions were as described (Sherman and Brophy, 2000).

Acknowledgments

We thank Heather Anderson and Linda Ferguson for excellent assistance and B. Smith for technical support. Sue Fleetwood-Walker and Clare Proudfoot are thanked for their valuable advice. Generous gifts of antibodies from Drs. D.R. Colman, M. Komada, B. Ranscht, and M. Rasband are gratefully acknowledged. This work was supported by the Medical Research Council and the Wellcome Trust. The ISCR Gene Targeting Laboratory was supported by the UK Biotechnology and Biological Sciences Research Council.

Received: August 25, 2005

Revised: September 23, 2005

Accepted: October 7, 2005

Published: December 7, 2005

References

- Bennett, V., and Lambert, S. (1999). Physiological roles of axonal ankyrins in survival of premyelinated axons and localization of voltage-gated sodium channels. *J. Neurocytol.* **28**, 303–318.
- Bhat, M.A., Rios, J.C., Lu, Y., Garcia-Fresco, G.P., Ching, W., St Martin, M., Li, J., Einheber, S., Chesler, M., Rosenbluth, J., et al. (2001). Axon-glia interactions and the domain organization of myelinated axons requires neuexin IV/Caspr/Paranodin. *Neuron* **30**, 369–383.
- Boiko, T., Rasband, M.N., Levinson, S.R., Caldwell, J.H., Mandel, G., Trimmer, J.S., and Matthews, G. (2001). Compact myelin dictates the differential targeting of two sodium channel isoforms in the same axon. *Neuron* **30**, 91–104.
- Boyle, M.E., Berglund, E.O., Murai, K.K., Weber, L., Peles, E., and Ranscht, B. (2001). Contactin orchestrates assembly of the septate-like junctions at the paranode in myelinated peripheral nerve. *Neuron* **30**, 385–397.
- Charles, P., Tait, S., Faivre-Sarrailh, C., Barbin, G., Gunn-Moore, F., Denisenko-Nehrbass, N., Guennoc, A.M., Girault, J.A., Brophy, P.J., and Lubetzki, C. (2002). Neurofascin is a glial receptor for the paranodin/Caspr-contactin axonal complex at the axoglial junction. *Curr. Biol.* **12**, 217–220.
- Court, F.A., Sherman, D.L., Pratt, T., Garry, E.M., Ribchester, R.R., Cottrell, D.F., Fleetwood-Walker, S.M., and Brophy, P.J. (2004). Restricted growth of Schwann cells lacking Cajal bands slows conduction in myelinated nerves. *Nature* **431**, 191–195.
- Custer, A.W., Kazarinova-Noyes, K., Sakurai, T., Xu, X., Simon, W., Grumet, M., and Shrager, P. (2003). The role of the ankyrin-binding protein NrCAM in node of Ranvier formation. *J. Neurosci.* **23**, 10032–10039.
- Davis, J.Q., and Bennett, V. (1993). Ankyrin-binding activity of nervous system cell adhesion molecules expressed in adult brain. *J. Cell Sci. Suppl.* **17**, 109–117.
- Davis, J.Q., Lambert, S., and Bennett, V. (1996). Molecular composition of the node of Ranvier: identification of ankyrin-binding cell adhesion molecules neurofascin (mucin+/third FNIII domain-) and NrCAM at nodal axon segments. *J. Cell Biol.* **135**, 1355–1367.
- Einheber, S., Zanazzi, G., Ching, W., Scherer, S., Milner, T.A., Peles, E., and Salzer, J.L. (1997). The axonal membrane protein Caspr, a homologue of neuexin IV, is a component of the septate-like paranodal junctions that assemble during myelination. *J. Cell Biol.* **139**, 1495–1506.
- Eshed, Y., Feinberg, K., Poliak, S., Sabanay, H., Sarig-Nadiri, O., Spiegel, I., Bermingham, J.R., Jr., and Peles, E. (2005). Gliomedin mediates schwann cell-axon interaction and the molecular assembly of the nodes of ranvier. *Neuron* **47**, 215–229.
- Faivre-Sarrailh, C., Gauthier, F., Denisenko-Nehrbass, N., Le Bivic, A., Rougon, G., and Girault, J.A. (2000). The glycosylphosphatidylinositol-anchored adhesion molecule F3/contactin is required for surface transport of paranodin/contactin-associated protein (caspr). *J. Cell Biol.* **149**, 491–502.
- Gillespie, C.S., Sherman, D.L., Blair, G.E., and Brophy, P.J. (1994). Periaxin, a novel protein of myelinating Schwann cells with a possible role in axonal ensheathment. *Neuron* **12**, 497–508.
- Gillespie, C.S., Sherman, D.L., Fleetwood-Walker, S.M., Cottrell, D.F., Tait, S., Garry, E.M., Wallace, V.C., Ure, J., Griffiths, I.R., Smith, A., and Brophy, P.J. (2000). Peripheral demyelination and neuropathic pain behavior in periaxin-deficient mice. *Neuron* **26**, 523–531.
- Gollan, L., Salomon, D., Salzer, J.L., and Peles, E. (2003). Caspr regulates the processing of contactin and inhibits its binding to neurofascin. *J. Cell Biol.* **163**, 1213–1218.
- Jenkins, S.M., and Bennett, V. (2002). Developing nodes of Ranvier are defined by ankyrin-G clustering and are independent of paranodal axoglial adhesion. *Proc. Natl. Acad. Sci. USA* **99**, 2303–2308.
- Komada, M., and Soriano, P. (2002). [Beta]IV-spectrin regulates sodium channel clustering through ankyrin-G at axon initial segments and nodes of Ranvier. *J. Cell Biol.* **156**, 337–348.
- Lacas-Gervais, S., Guo, J., Strenzke, N., Scarfone, E., Kolpe, M., Jahkel, M., De Camilli, P., Moser, T., Rasband, M.N., and Solimena, M. (2004). BetaIVSigma1 spectrin stabilizes the nodes of Ranvier and axon initial segments. *J. Cell Biol.* **166**, 983–990.
- Lambert, S., Davis, J.Q., and Bennett, V. (1997). Morphogenesis of the node of Ranvier: co-clusters of ankyrin and ankyrin-binding integral proteins define early developmental intermediates. *J. Neurosci.* **17**, 7025–7036.
- Lustig, M., Zanazzi, G., Sakurai, T., Blanco, C., Levinson, S.R., Lambert, S., Grumet, M., and Salzer, J.L. (2001). Nr-CAM and neurofascin interactions regulate ankyrin G and sodium channel clustering at the node of Ranvier. *Curr. Biol.* **11**, 1864–1869.
- McEwen, D.P., and Isom, L.L. (2004). Heterophilic interactions of sodium channel beta1 subunits with axonal and glial cell adhesion molecules. *J. Biol. Chem.* **279**, 52744–52752.
- Menegoz, M., Gaspar, P., Le Bert, M., Galvez, T., Burgaya, F., Palfrey, C., Ezan, P., Arnos, F., and Girault, J.A. (1997). Paranodin, a glycoprotein of neuronal paranodal membranes. *Neuron* **19**, 319–331.
- Pedraza, L., Huang, J.K., and Colman, D.R. (2001). Organizing principles of the axoglial apparatus. *Neuron* **30**, 335–344.
- Poliak, S., and Peles, E. (2003). The local differentiation of myelinated axons at nodes of Ranvier. *Nat. Rev. Neurosci.* **4**, 968–980.
- Ranvier, L. (1875). *Traite Technique d'Histologie* (Paris: F. Savy).
- Sakurai, T., Lustig, M., Babiarz, J., Furley, A.J., Tait, S., Brophy, P.J., Brown, S.A., Brown, L.Y., Mason, C.A., and Grumet, M. (2001). Overlapping functions of the cell adhesion molecules Nr-CAM and L1 in cerebellar granule cell development. *J. Cell Biol.* **154**, 1259–1273.
- Salzer, J.L. (2003). Polarized domains of myelinated axons. *Neuron* **40**, 297–318.
- Sherman, D.L., and Brophy, P.J. (2000). A tripartite nuclear localization signal in the PDZ-domain protein L-periaxin. *J. Biol. Chem.* **275**, 4537–4540.
- Sherman, D.L., and Brophy, P.J. (2005). Mechanisms of axon ensheathment and myelin growth. *Nat. Rev. Neurosci.* **6**, 683–690.
- Tait, S., Gunn-Moore, F., Collinson, J.M., Huang, J., Lubetzki, C., Pedraza, L., Sherman, D.L., Colman, D.R., and Brophy, P.J. (2000). An oligodendrocyte cell adhesion molecule at the site of assembly of the paranodal axo-glia junction. *J. Cell Biol.* **150**, 657–666.
- Vouyiouklis, D.A., and Brophy, P.J. (1993). Microtubule-associated protein MAP1B expression precedes the morphological differentiation of oligodendrocytes. *J. Neurosci. Res.* **35**, 257–267.
- Wight, P.A., Duchala, C.S., Readhead, C., and Macklin, W.B. (1993). A myelin proteolipid protein-LacZ fusion protein is developmentally regulated and targeted to the myelin membrane in transgenic mice. *J. Cell Biol.* **123**, 443–454.